

Supplementary Information for manuscript

Magmatic degassing and fluid metasomatism promote compositional variation from I-type to peralkaline A-type granite in late Cretaceous Fuzhou felsic complex, SE China

Feng Zhang^{1,2,3}, Feng Guo^{1,2*}, Xiaobing Zhang^{1,2}, Liang Zhao^{1,2}

1 State Key Laboratory of Isotope Geochemistry, Guangzhou Institute of Geochemistry, Chinese Academy of Sciences, Guangzhou 510640, China

2 Chinese Academy of Sciences Center for Excellence in Deep Earth Science, Guangzhou 510640, China

3 College of Earth and Planetary Sciences, University of Chinese Academy of Sciences, Beijing 10100049, China

*** Corresponding author, email: guofengt@263.net**

Supplementary Figures

In order to make the manuscript concise and avoid repetitions from the literature, we also place the additional six figures in the Supplementary Information as supplementary figures (Figs. S1-6).

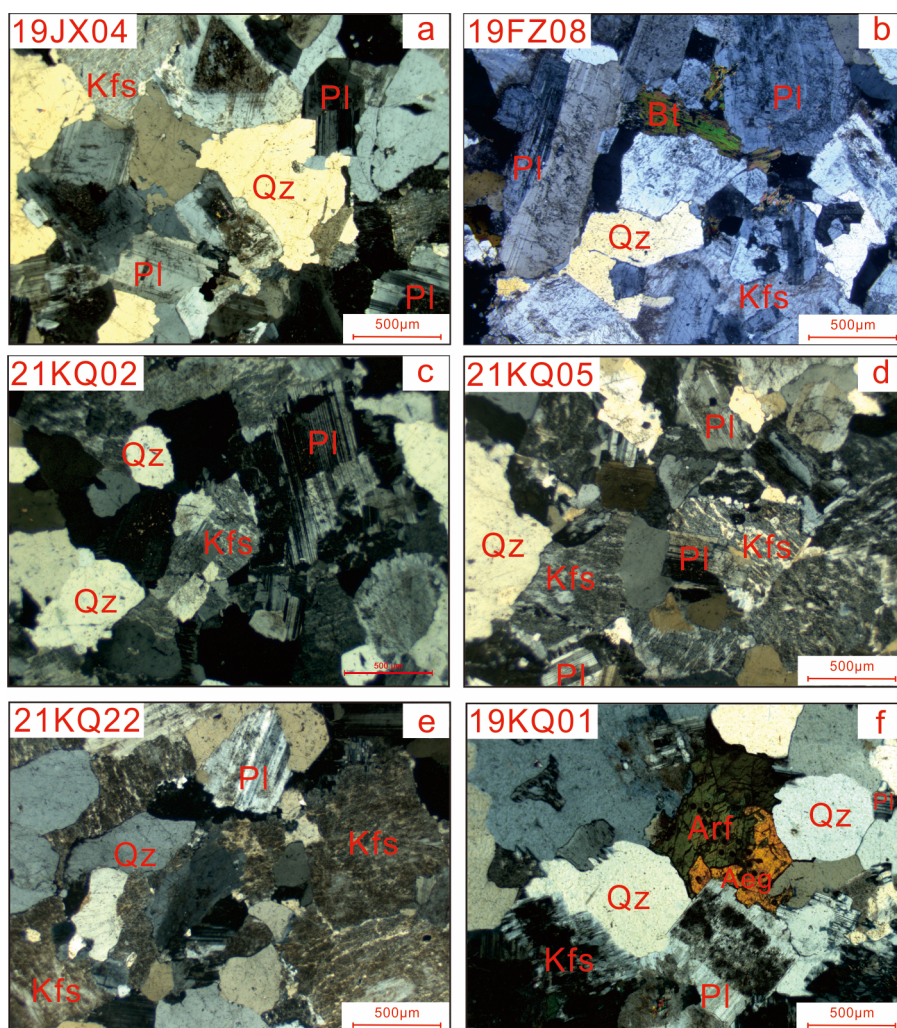


Figure S1 Representative microphotos of the Fuzhou I-A-type granitic complex (a-f).

Photos (a, b) show the mineral assemblage and microstructure of I-type granites and photos (c-f) show the mineral assemblage and microstructure of A-type granite. Mineral abbreviations: Pl – plagioclase; Kfs – K-feldspar; Qtz – quartz; Bt – biotite; Arf – arfvedsonite; Aeg – aegirine.

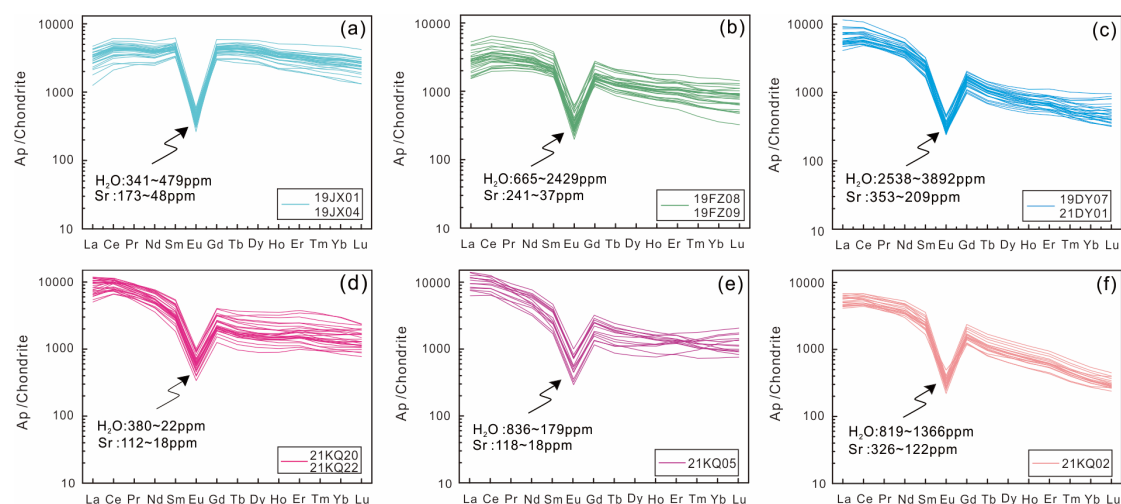


Figure S2 Chondrite-normalized REE spidergrams of apatite in the I-type granitoids (a-c) and A-type granites (e-f). Following the decrease of Sr and H_2O , the apatite crystals in I-type granitoids and A-type granites show different evolution trends. See details in the text.

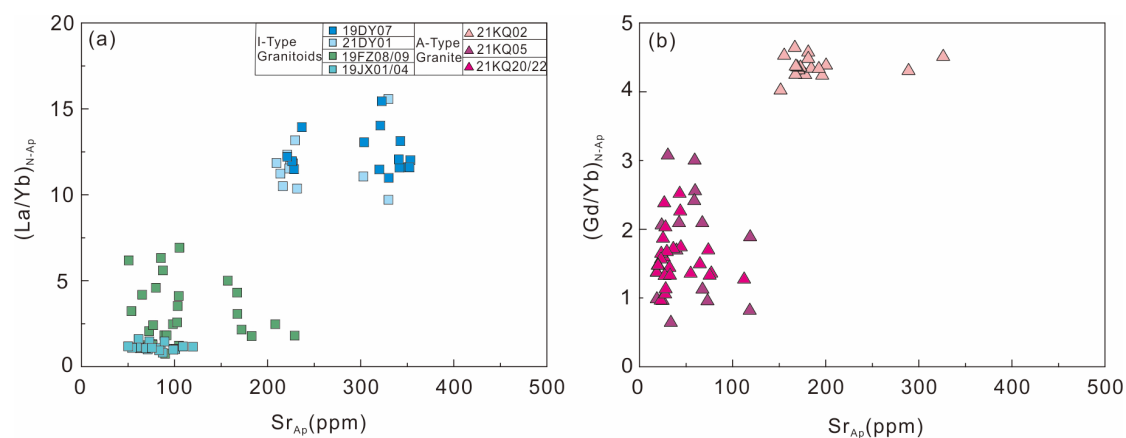


Figure S3 Apatite Sr concentrations plotted against $(La/Yb)_N$ from I-type granitoids (a) and $(Gd/Yb)_N$ from A-type granite (b). In (a), a roughly positive correlation between Sr and $(La/Yb)_N$ in apatite indicates the fractionation of plagioclase and apatite. In (b), the HREE fractionation expressed as $(Gd/Yb)_N$ becomes weaker following a decrease of Sr in apatite. Please also see details in the text.

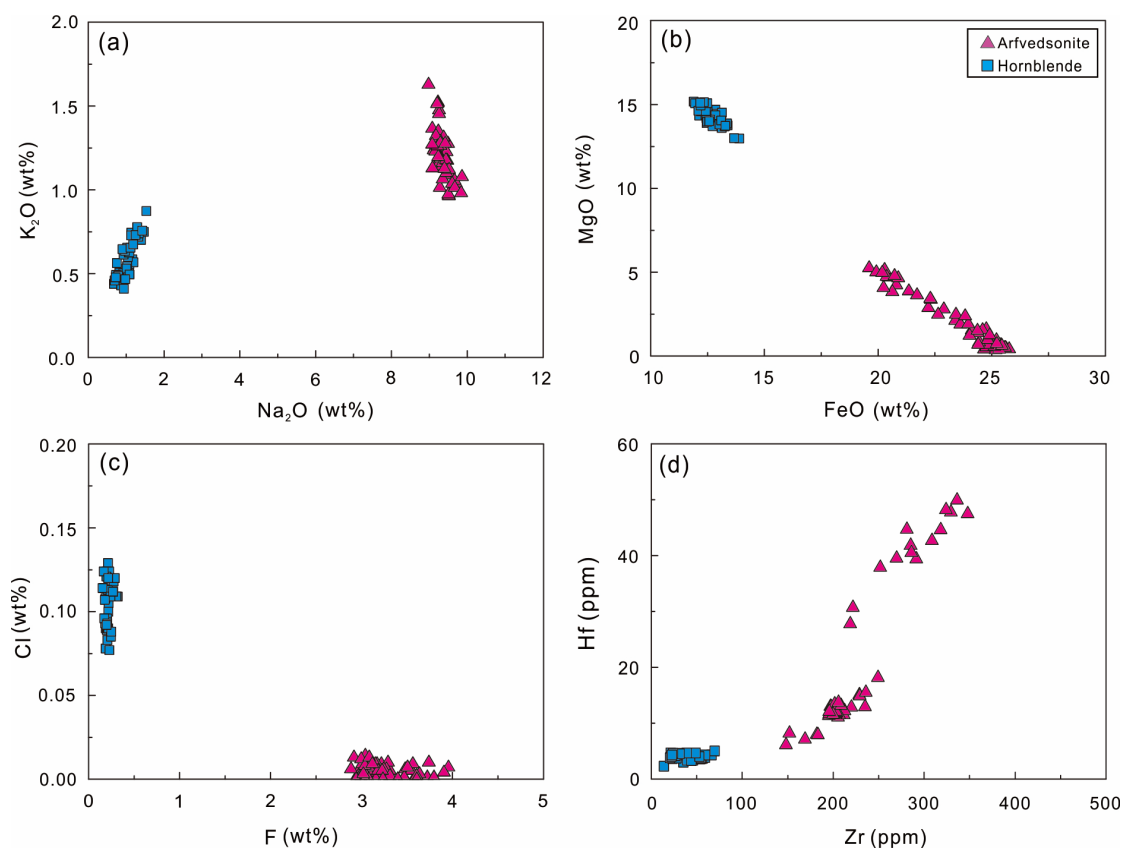


Figure S4 Diagrams of Na₂O versus K₂O (a), FeO versus MgO (b), F versus Cl (c) and Zr versus Hf (d) of hornblende and arfvedsonite respectively from the I-type granitoids and A-type granites. See details in the text.

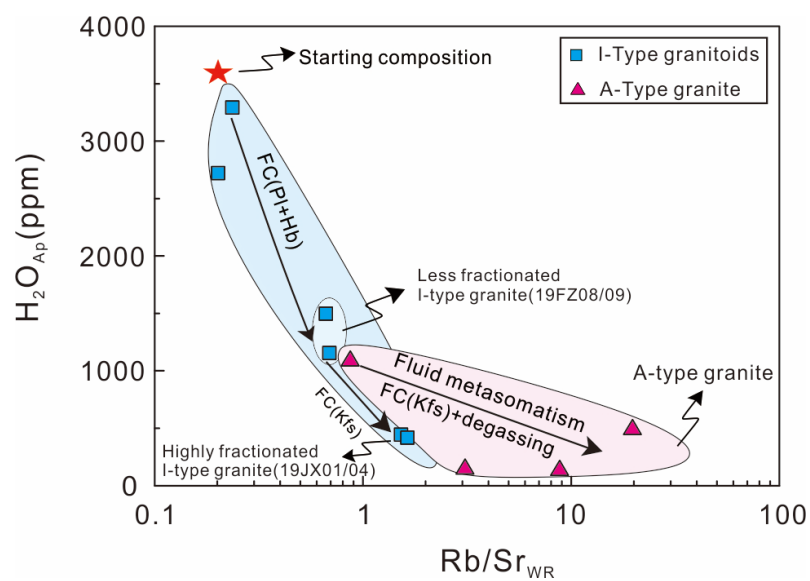


Figure S5 Diagrams of H₂O content of apatite versus whole-rock Rb/Sr.

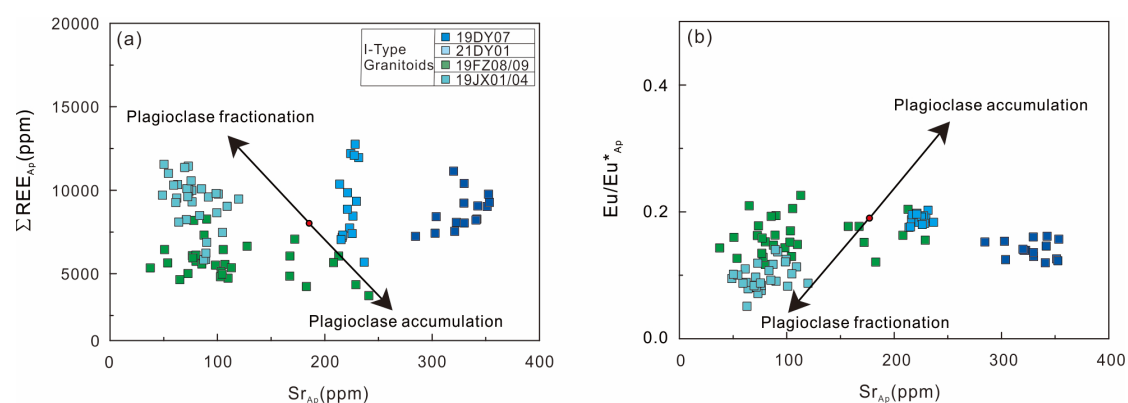


Figure S6 Diagrams of apatite Sr versus ΣREE (a) and Eu/Eu^* (b), precluding a significant role of plagioclase accumulation.

Table 1 Partition coefficients (K_d) used in Figure 8

Element/ K_d	K-feldspar	Hornblende	Plagioclase	Biotite	Apatite	Zircon
Rb	0.07	0.02	0.13	2.46	0.1	0.01
Ba	18.0	0.92	4.0	5.0	0.1	0.01
K	2.0	0.01	0.01	0.19	0.1	0.01
Nb	0.1	1.5	0.07	4.6	0.1	0.01
Sr	6.0	1.13	10.0	0.53	2.4	0.01
Zr	0.01	0.53	0.20	0.79	0.1	2800
Hf	0.02	0.52	0.03	0.44	0.1	2645
La	0.15	0.36	0.30	2.59	10	26
Nd	0.04	1.6	0.19	4.0	60	22
Eu	3.0	3.2	2.0	4.7	15	20
Yb	0.1	1.8	0.1	0.6	50	490

Note: partition coefficients (K_d) are from website: <http://earthref.org/KdD/>.

References:

Stephant, A., Anand, M., Tartèse, R., Zhao, X., Degli-Alessandrini, G., and Franchi, I.

A. (2020) The hydrogen isotopic composition of lunar melt inclusions: An interplay of complex magmatic and secondary processes. *Geochimica et Cosmochimica Acta*, 284,196–221.